J Mater Sci (2016) 51:4061–4069
DOI 10.1007/s10853-016-9726-9

Domain structure and polarization reversal in ferroelectric lanthanum-modified lead titanate ceramics investigated by piezoresponse force microscopy

André Marino Gonçalves[1] · Fernando Andres Londono[1,2] · Ducinei Garcia[1] · José Antonio Eiras[1]

Received: 8 October 2015 / Accepted: 4 January 2016 / Published online: 13 January 2016

Abstract In this work, the ferroelectric domain structure of $(Pb_{0.79}La_{0.21})TiO_3$ transparent ceramics and its response to an applied electric field were investigated by piezoresponse force microscopy (PFM). A qualitative three-dimensional reconstruction of the domains by PFM measurements revealed that the domain structure consists in stripes in two size scales (micro and nanometer) separated by 90° domain walls coexisting with 180° domains. While the nanoscale 90° domains were found arranged in organized structures, (e.g., lamellas, herringbones, and other unusual configurations), the 180° domains form a "labyrinth" structure, typical of ferroelectrics with a degree of disorder. Local application of an electric field reveals different coercive voltages to reorient 180° and the two types of 90° domains and the appearance of a different nanoscale 90° domain structure after poling. While the labyrinth structure is destroyed with relative low voltages, the created 90° domains structure persists, avoiding the formation of a single-domain structure.

Introduction

Ferroelectric domain structures have been studied a long time by techniques such as chemical etching and optical or scanning electron microscopy. In ceramics, a series of works performed specially by Arlt [1, 2] showed a dependence law of the domain width w with the grain size g, as $w \propto g^{1/2}$. Actually, not only the size, but also the configuration of the ferroelectric/ferroelastic domains are dependent of the grain size, changing at critical sizes to states as "herringbones," lamellas or also single-domain states [1].

With the advent of new techniques, in which piezoresponse force microscopy (PFM) takes one of the most important roles, the research in ferroelectric domains experienced a revival [3–5], leading to the discovery of novel geometries and domains organization [6, 7], as well as the response of them under external electric fields, both macro or locally applied [8–10]. Despite the steady growth in this subject, most of the works are being performed in single crystals and epitaxial thin films, especially due to difficulties in the correct interpretation of PFM signals in polycrystalline media [11, 12].

Lanthanum-modified Lead Titanate (PLT) ferroelectric ceramics have emerged as highly promising materials for piezo-mechanical and pyroelectric applications, owing to their high electromechanical anisotropy factor and large pyroelectric coefficient along the polarization axis, respectively [13, 14]. Besides that, it was shown that ferroelectric transparent ceramics of PLT have good optical and electro-optical properties, which makes it a good candidate for electro-optical component in optical waveguides, for example [15, 16]. Although all these properties are related to the ferroelectric domain properties, few works had been devoted in investigating its configuration [17–20]. In ceramics, the domain structure of the PLT system was studied by transmission electron microscopy (TEM) [21–23], showing a strong dependence on lanthanum concentration, evaluating from classical stripe ferroelectric domains to a typical relaxor polar

✉ André Marino Gonçalves
andre@df.ufscar.br

[1] Ferroic Materials Group, Department of Physics, Federal University of São Carlos, São Carlos, SP 13565-905, Brazil

[2] Institute of Physics, Universidad de Antioquia, Medellin, Colombia

nanodomains configuration, when adding lanthanum. However, a detailed outlook of the domain structure was not accomplished, due to the limitation of the techniques.

In this sense, PFM has the great advantage of being sensitive to the polarization direction and to probe both out-of-plane and in-plane components of the piezoresponse, thus, allowing a three-dimensional reconstruction of the domains structure. Furthermore, the response of PLT domains to external applied electric fields, which can be extensively explored in PFM, was subject of only few works [19, 20], and information in this matter is still lacking. In this work, the domain structure of tetragonal $(Pb_{0.79}La_{0.21})TiO_3$ transparent ceramics was investigated in detail by means of PFM. A qualitative three-dimensional reconstruction of the orientation of the domains was achieved and the response with local application of electric fields was also investigated.

Materials and methods

High-quality transparent $(Pb_{0.79}La_{0.21})TiO_3$ (PLT21) ferroelectric ceramics were prepared by solid-state reaction and conventional sintering. Details of the synthesis process may be found elsewhere [15]. After polishing with 3 μm diamond paste, the ceramics were thermally etched in air at 1100 °C, for 1 min in a sealed alumina crucible for revealing the grains. Atomic (AFM) and Piezoresponse (PFM) Force Microscopy experiments were carried in a Shimadzu SPM 9600, with internal signal generator and lock-in, adapted for PFM measurements.

The PFM images were obtained recording the X-output signal from the lock-in. Pt/Ir-coated probes (PPP-EFM, from Nanosensors), with a force constant of 2.8 N/m, were utilized for the measurements with exciting voltage of 4 V_{pk} at 35 kHz. This probing frequency was empirically chosen, but far from any resonance. The out-of-plane component of piezoresponse were also obtained at 330 kHz. This frequency, also empirically chosen, is near the contact resonance and gives a better signal/noise ratio. In these cases, the images obtained far and near the resonance were compared, in order to avoid misinterpretation due to topography artifacts.

To perform the qualitative three-dimensional reconstruction of the relative domains orientation, after imaging the out-of-plane and in-plane components of the piezoresponse, the sample was manually rotated by 90° and a new in-plane image of the same region was taken. In the qualitative reconstruction, the absolute magnitude of the polarization is not measured, thus the polarization cannot be combined vectorially. However, the direction of the three components of the polarization in each domain is identified and also the relative magnitude of the polarization in different domains can be compared in each image. With this information and the knowledge of the crystallographic symmetry of the sample, the polarization was reconstructed in a qualitative map (see Fig. 2e).

In our results the following convention was adopted, which is shown in Fig. 1. In each PFM image, there is a cantilever schematized (Fig. 1a) showing the direction of the probed piezoresponse, and the color representing the maximum piezoresponse of each direction. Different shades of gray are related with intermediate intensities of piezoresponse in the probed region as shown in Fig. 1b, c. Whenever the cantilevers are not shown, all the images correspond to the Z probed direction.

Results

Original domain configuration

Figure 2a–c shows the PFM images obtained in the region shown in Fig. 2d. Three main features are observed in these images, which are representative to the entire sample. First, domains with opposite piezoresponse, i.e., bright and dark colors in PFM, which correspond to ferroelectric 180° domains, are seen in the entire grain. The interface of these 180° domains are not only straight lines, but also forms a labyrinth-shaped pattern. Antiparallel domains are unambiguously identified in PFM, even without knowing the crystallographic orientation, by an inversion of the phase of the three components of piezoresponse, as shown in Fig. 2e.

The second feature of the domains structure are the long stripes with different PFM intensities, which often have more than 1 μm width, and a length that can cross the entire grain. Five of these are indicated by numbers in Fig. 2a, b. Stripes with more PFM intensity in Fig. 2a (Z laboratorial direction) are different from those in Fig. 2b (X direction), which means that stripes 1, 3, and 5 have the polarization lying more in the out-of-plane direction, while stripes 2 and 4 in the in-plane direction. By analyzing cross section profiles passing through two stripes, we concluded

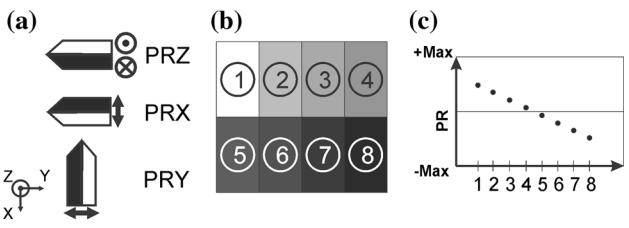

Fig. 1 Convention utilized in PFM images **a** cantilevers showing the direction of the probed piezoresponse, **b** color map representing a PFM image, and **c** piezoresponse intensities corresponding to the regions in (**b**)

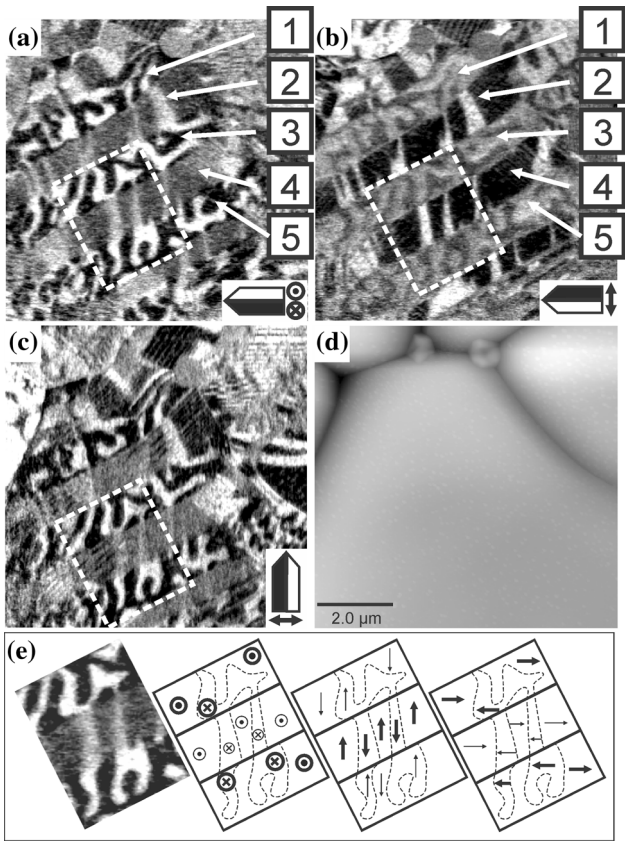

Fig. 2 Qualitative three-dimensional reconstruction of domains configuration in PLT21 probed by PFM **a** out-of-plane (Z), **b** in-plane (X), and **c** in-plane (Y) components of piezoresponse obtained in the region shown in the topography image in (**d**). The numbers *1–5* in (**a**) and **b** shows five mesoscale domains separated by 90° walls. **e** is a scheme of the polarization components of the region demarked by the dashed rectangle. The different PFM intensities in each image are differentiated by the thickness of the *arrows*. The *dashed curves* and *solid lines* inside each *rectangle demarcates* the 180° and 90° walls respectively

that they are domains separated by 90° walls. A main point is that antiparallel domains have different degrees of order in different stripes, i.e., the 180° domain walls within the stripes 2 and 4 (in-plane polarization) are straighter than those within the stripes 1, 3, and 5 (out-of-plane polarization).

The last feature that can be observed in Fig. 2 and with more details, in Fig. 3, is the nanoscale 90° domains, observed as small stripes that appear in many regions of the grain. These kind of domains mostly arrange themselves as the classical description of the A, B, and C DWs (tetragonal c-axis, makes an angle of 45° with the A and B DWs normal vector and 90° with C DWs normal vector) [2]. In the description of [2], these three kinds of domain walls appear organized in configurations such as lamellas and herringbones. In our observations, such kind of configurations were indeed observed (see Fig. 3c), however other

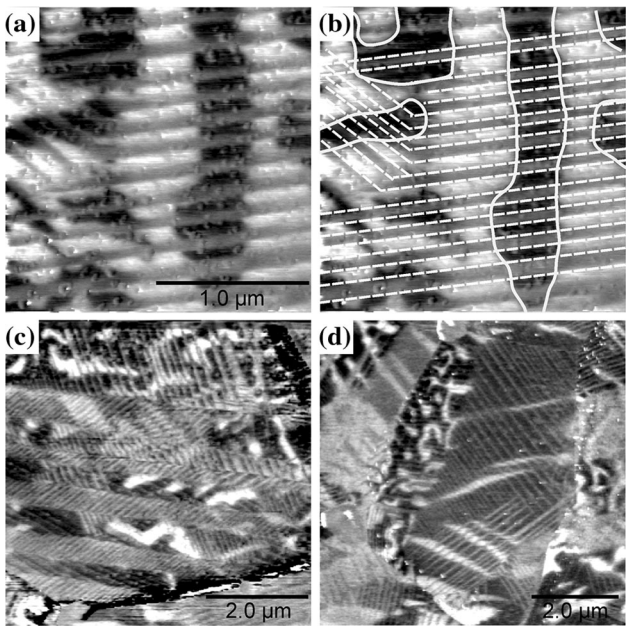

Fig. 3 Nanoscale 90° domains walls (DWs) **a** out-of-plane (Z) piezoresponse of a region showing nanoscale 90° domains. In **b**, the same region shown in **a** superimposed by dashed lines delimiting 90° DWs and *solid lines* delimiting 180° DWs. **c** out-of-plane image of a different region showing classical arrangements of lamellas and "herringbones" formed by the nanoscale 90° DWs. **d** out-of-plane image of a third region showing unusual arrangements

unusual configurations formed by the nanoscale 90°domains were also found (Fig. 3d).

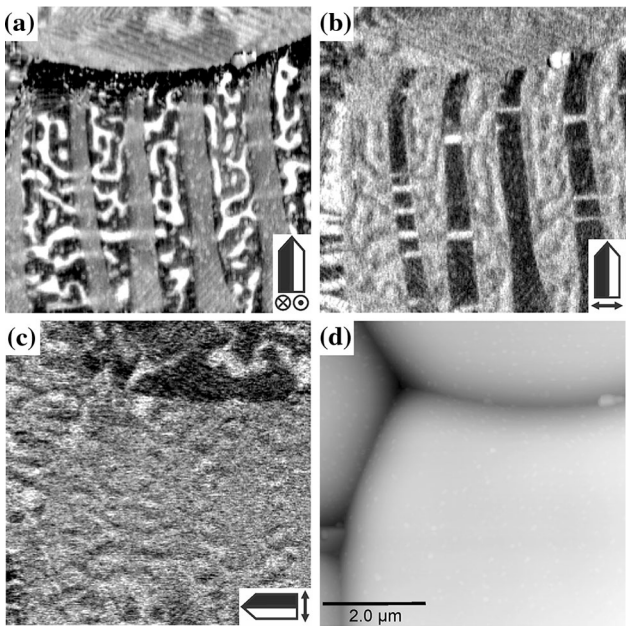

Fig. 4 Observation of different orders of 180° domains walls in out-of-plane and in-plane domains **a** out-of-plane (Z), **b** in-plane (Y), and **c** in-plane (X) components of piezoresponse obtained in the region shown in the topography image in (**d**)

Figure 4 shows another region of the sample exhibiting the same three representative features. Note that similar to the images in Fig. 2, the 180° domains with in-plane polarization have straighter DWs than those with out-of-plane polarization. This region, however, was scanned in a way that the piezoresponse-probed directions in the in-plane images were parallel (Fig. 4b) and perpendicular (Fig. 4c) to the domains walls. In Fig. 4c, a null piezoresponse is observed, which means that the in-plane component of the polarization vector is completely oriented parallel to the domain walls.

Response to electric field

The response and reconfiguration of the ferroelectric domain structure under an applied electric field were also studied. In this case, a region of the sample (virgin state) under investigation was probed before applying a bias field, and after that, the same region (or a sub-region) was scanned while applying a dc voltage, in the order of several tens of volts. Finally, the bias was turned off and a new piezoresponse measurement was performed. Note that when the field is applied direct on the surface of the sample (not on an electrode), very high electric fields are obtained, due to the spherical aspect and low dimensions of the tip, making possible the reorientation of the polarization with relative low voltages.

Figure 5 shows the evolution of the domain configuration after several applied voltages. In Fig. 5b we can observe the original domain configuration showing the typical three features described in the previous session. Here, the stripes 2 and 4 are composed by domains with polarization lying more in the out-of-plane direction, (parallel to the applied field). For sake of simplicity, we will call these stripes, OP domains. Stripes 1, 3, and 5, on the other hand, are composed by domains with polarization lying most on the in-plane direction (perpendicular to the applied field), which will be denominated IP domains. The dashed square in Fig. 5b denotes the region where the bias dc voltage was applied.

After applying +30 V (Fig. 5c), the destruction of the labyrinth type structure, and the switching of both OP and IP domains to the same direction of polarization (bright color) can be observed. The reorientation of the original domain structure is followed by the appearance of a new configuration of 90° domains (gray stripes), whose size and organization are different from both the meso- and nanoscale domains that had been spontaneously formed in the sample. After applying in the same region −30 V (Fig. 5d), we can observe the switching to the inverse direction of polarization (dark color), with the creation of new 90° domains, organized in a distinct way than of those for +30 V applied field. Voltages up to −60 V were not sufficient to induce a single-domain state (Fig. 5e, f), just only slight differences in domains appears, remaining the same main configuration.

Figure 6 shows a region of the sample that shows a different evolution of domains than the observed in Fig. 5. In images (c-f), the poling processes was performed applying a negative voltage in the upper half and a positive voltage in the lower half. Utilizing the same criteria, we name stripes 1 and 3 as OP domains and stripe 2 as IP domain. After applying −30 V (Fig. 6c), we can observe in the upper half of the image, the switching of OP domains, i.e., 180° domains were all switched to the same direction, with destruction of the labyrinth type structure and the appearance of a new 90° nanoscale domain configuration. Differently from the results shown in Fig. 5, the IP domain remained with the in-plane orientation. However, we can see that even inside the IP stripe, the 180° domains were all oriented to the same in-plane direction with the application of −30 V. This can be observed by the disappearance of the small contrast after applying the bias voltage (compare stripe 2 in Fig. 6b, c). Previous results in our group show that in the local poling process, the polarization orientation of the domains follows the movement of the biased tip, in both the fast- and slow-scan direction, in such a way that the polarization tends to remain oriented in the direction where the tip stops the scanning [24].

By progressively increasing the applied voltage, we can observe with −40 V (Fig. 6d) the growth of the OP domains and reduction of the IP domain, while with −50 V (Fig. 6e), there is a nucleation of an out-of-plane domain inside the IP domain. After applying −60 V, almost all the selected region was reoriented to the out-of-plane direction.

Unexpectedly, the lower half of Fig. 6c–f, where positive voltage was applied, showed a different behavior, compared to the upper figures, apparently showing a full switching of polarization. However, this was not a representative observation, i.e., the same poling process was performed several tens of time in different regions of the sample, and no other observation of this kind was made.

Discussion

The domains structure found in $(Pb_{0.79}La_{0.21})TiO_3$ (PLT21) consists in an arrangement of two length-scales 90° domains and labyrinthine 180° domains. As shown in detail in Fig. 3, the 90° and 180° domain wall cross each other, yielding rather complex domains patterns.

The 90° domains show a very well-ordered structure, in both meso- and nanoscale. In mesoscale, only straight stripes are observed, which often have 1 μm of width and length that can cross the entire grain. At nanoscale, the domains have around 100 nm, and were arranged in very

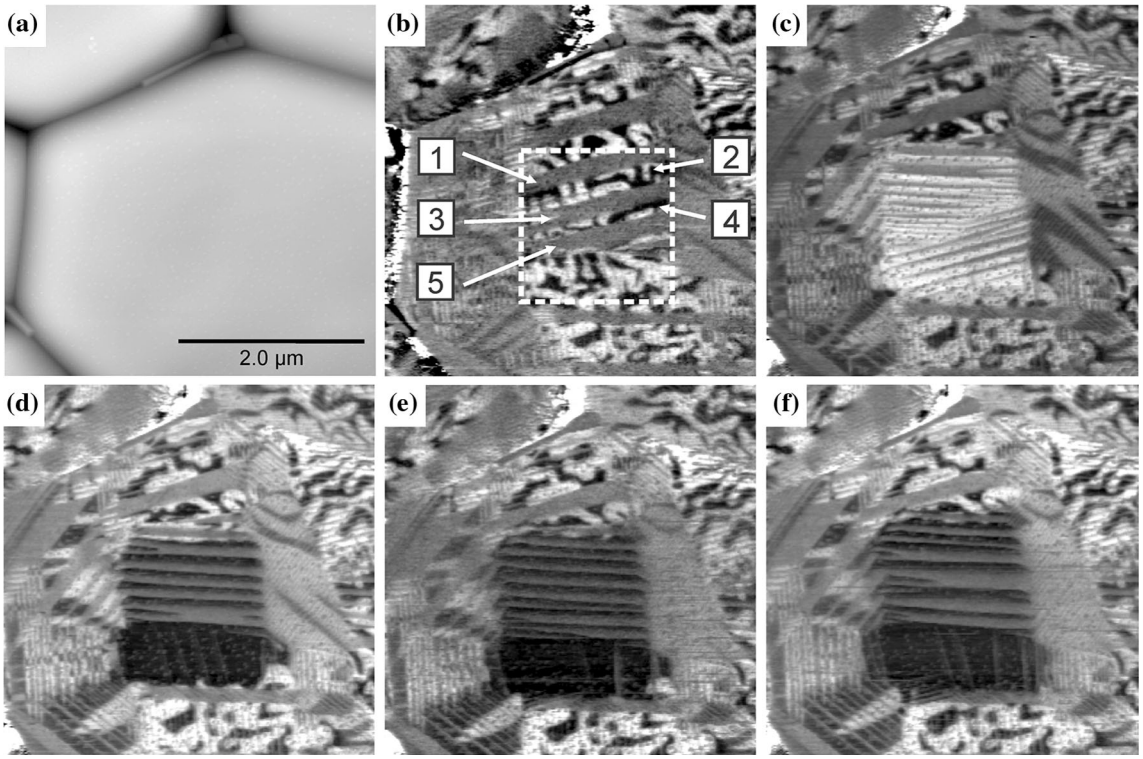

Fig. 5 Evolution of domains configuration with applied electric field. **a** topography; and **b** out-of-plane piezoresponse image of the original state of domains. **c–f** out-of-plane piezoresponse images of the same region **a** after applying **c** +30 V, **d** −30 V, **e** −45 V, and **f** −60 V in the region delimited by the *dashed square* in (**b**)

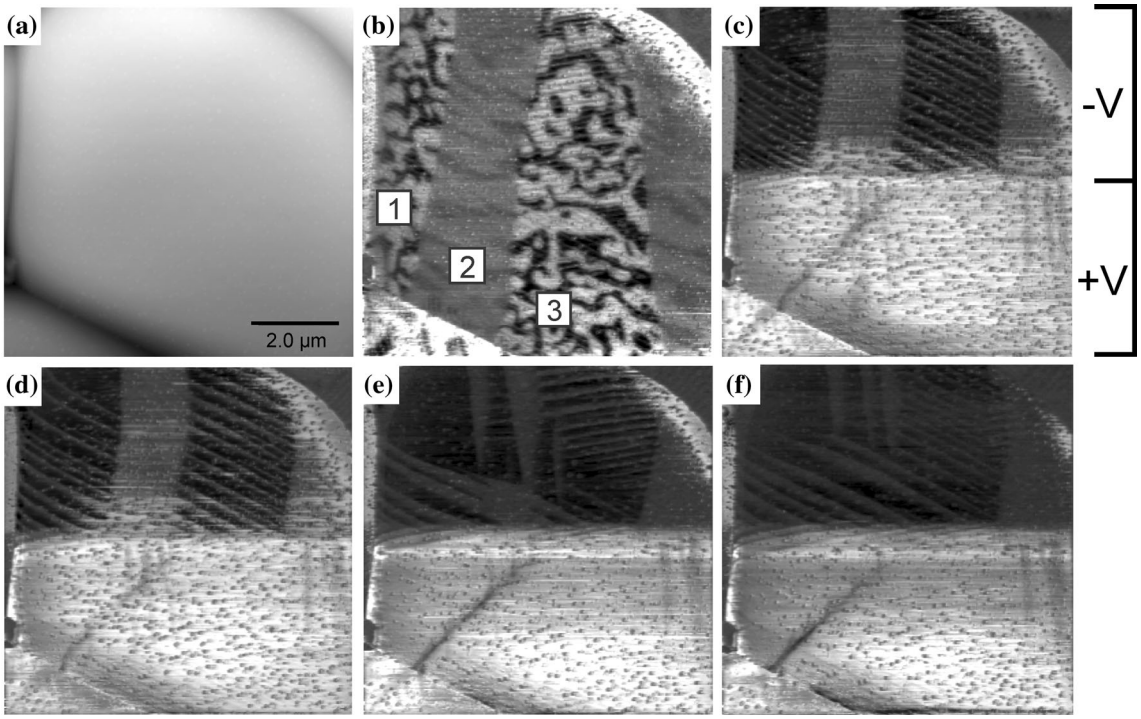

Fig. 6 Evolution of domains configuration with applied electric field. **a** topography and **b** out-of-plane piezoresponse image of the virgin state of domains. **c–f** out-of-plane piezoresponse images of the same region **a** after applying **c** ±30 V, **d** ±40 V, **e** ±50 V, and **f** ±60 V, with negative voltage in the *upper half* and positive voltage in the *lower half*, as schematized in (**c**)

well-known structures such as lamellas and herringbones (Fig. 3c) and also in other unusual structures that consist in different arrangements of bundles of 90° walls (Fig. 3d). Similar observations of these unusual structures were made in polycrystalline ferroelectric thin films [6]. The explanation is that these configurations of the domains might be more effective in minimizing the electromechanical energy than the classical lamellas and herringbones configuration, even with the cost of forming charged domain walls (CDWs) [6].

The 180° domains show a more complex structure with different degrees of order within different 90° stripes. Antiparallel domains with polarization lying more in the in-plane direction are much more ordered (i.e., their 180° walls are much straighter) than those with polarization lying more in the out-of-plane direction. This can be explained by the assumption that the ferroelectric 180° domains are stabilized in a way to suppress the formation of CDWs. 180° domains are not ferroelastic, and in the absence of critical conditions will stabilize in an electrically neutral configuration of the walls.

Let us assume that we are probing a domain wall of two antiparallel c-domains, (Fig. 7a, left side). In this case, no matter the orientation of the wall, it will always correspond to a non-CDW (Fig. 7b, left side). However, if we consider a domain wall separating two antiparallel a-domains as in the right side of Fig. 7a, the only configuration that corresponds to a non-CDW is the one in which the wall is parallel to the direction of polarization (Fig. 7b, right side). For this reason, the in-plane 180° domains, probed in the sample surface, as observed in Fig. 4b, show straighter walls, and in consequence an apparent high degree of order, than the out-of-plane 180° domains (Fig. 4a).

With the consideration described above, we can depict a scenario of the bulk domain configuration. In Fig. 8, we described a sample containing a cylindrical domain with

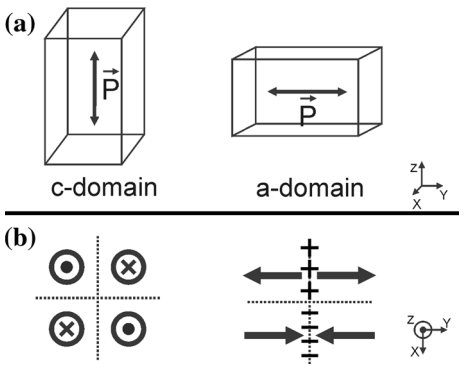

Fig. 7 Schematic of **a** c-domain and a-domain tetragonal cells, and **b** correspondent visualization of different possible types of domains walls probed in the surface of the sample. (+) and (−) signs show the formation of charged domain walls

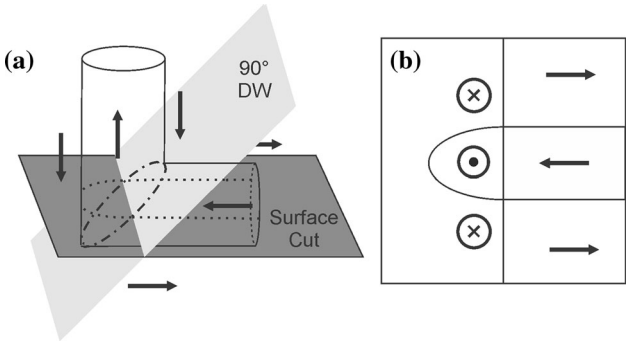

Fig. 8 Probing out-of-plane and in-plane domains **a** represents a domain structure with 180° and 90° domain walls, where the *arrows* represent the polarization vector. The *light gray plate* is the 90° domain wall plane and the *dark gray plate* is the cut where the PFM image in **b** is probed

opposite polarization from the surrounding region, crossing over a 90° domain wall. Supposing this sample were cut in (or polished until) the plane containing the dark gray plate, the corresponding polarization map of this surface would be that shown in Fig. 8b, which shows for the in-plane domains, walls as straight lines, and for the out-of-plane domains, curved walls. This pattern is the same that is observed in our PFM images. In Fig. 8, the simple case of a right circular cylinder domain within an antiparallel matrix is shown. All domains cannot be (simultaneously) right cylinders with circular or other regular bases, once this geometric configuration would not completely fill the space. However, it is straight ahead to construct domains as right cylinders with irregular bases, which fills the entire space and correctly reconstruct the PFM maps observed in Figs. 2, 3, and 4. The cylinder shape of the domains is directly related with the exclusion of head-to-head and tail-to-tail domain boundaries, which allows curved walls only in the out-of-plane direction.

Preview works had investigated the (Pb,La)TiO_3 system by TEM [21–23] and the authors agree in an evolution of the ferroelectric domain structure with the lanthanum concentration. First, in the region of low concentration of lanthanum, only classical micron-sized 90° domains are observed. Increasing the lanthanum concentration, an intermediate region of mixed micron-sized and fine (nanoscale) ferroelectric domains are found, until finally the system reaches a region with no evidence of ferroelectric domain walls, in which only a random local contrast is observed in TEM images and associated with polar nanodomains of the relaxor phase. Our observation is in accordance with these results, once PLT21 is in the intermediate region with micron and nano-sized 90° domains. However, the characteristic 180° domain structure found in our work were not clearly distinguished before. Although some evidences might be observed in TEM images

previously reported, we believe that these structures were not identified, because of the limitation of the techniques. For this kind of investigation, PFM has the great advantage of being strongly sensitive to the ferroelectric polarization, and able to unambiguously identify 180° domain walls.

Labyrinth arrangements of 180° nanodomains, similar to those shown in Figs. 2, 3, and 4, have recently been reported in single crystals and ceramics of pure relaxors and also compositions combining both relaxor and ferroelectric features (e.g., the solid-solution (1 − x)PMN-xPT) [25–28]. Its formation has been attributed to a competition between strain and electronic minimization of energy and random field effects, which breaks the long-range interaction of the domains [29].

Normal to relaxor transitions in PLT were found in compositions between 23 and 25 at.% [21, 30], thus the composition ($X = 21$) of lanthanum-modified lead titanate investigated in this work can be considered close to a relaxor ferroelectric composition, in which disorder effects could be acting in the shape and size of the domains. Concerning the shape, as we had shown, there is no electric constraint for the formation of irregular domain walls in the tetragonal c-axis direction, and the mechanisms for the formation of the labyrinth-shaped domain structure, could be, in principle, more general. In fact, micron-sized irregularly rounded domains with opposite polarization in the tetragonal c-axis were observed in the microstructure of $BaTiO_3$ single crystals and ceramics in the 1950s, and denominated as "watermarks" [31]. Even the end composition of PLT, $PbTiO_3$, observed by PFM presented the same irregular characteristics for the shape of the 180° domains [32]. On the other side, the width of few hundred nanometers of the ferroelectric domains is an evidence of the lanthanum concentration effect in reducing domain size, as already observed in other works.

The switching experiments show different coercive fields for the three kinds of domain in PLT21. In the case of 180° domains, a relatively small dc voltage were enough to reorient the polarization, and thus, destroy the labyrinth structure, as shown in Figs. 5 and 6. After each poling process, only classical 90° domain arrangements were found in the measurements.

Coercivity is a property that is dependent on the polarization anisotropy of the ferroelectric sample. In samples with high anisotropy, the polarization is strongly coupled to the lattice, so it is easier to switch 180° domains than to reorient 90° ones, because the latter involves a rotation of the polarization [33]. The evolution of the domain configuration with the magnitude of the applied field observed in Fig. 6 is very consistent with a model proposed by Ishibashi et al. for the polarization reorientation of 180° and 90° domain walls in a c/a/c-domain structure [34]. For low fields, only the 180° domains switch. For moderate fields, a growth of the out-of-plane domain and reduction of in-plane domains are observed. Finally, for strong fields, nucleation of out-of-plane domains inside the in-plane domain happens. According to [34], this behavior is characteristic of ferroelectrics with high polarization anisotropy.

On the other hand, different coercive voltages were also observed for the 90° reorientation of the nanoscale and mesoscale domains, and also, of mesoscale domains with different sizes (for example, lateral size of the IP domains in Figs. 5 and 6 are around 0.5 and 2 μm, respectively). This result gives us evidences about the relationship of the coercivity with the volume of the in-plane domains. However, a more detailed investigation, which was not in the scope of this work, must take in account that the geometry of the PFM is different from the parallel plate capacitor. Once the electric field is very concentrated at the tip, the effective field that the entire domain feels will be very dependent on the domain size.

All the poling processes performed in our study generated a new arrangement of 90° domain walls and a single-domain state was not achieved for any of the poling voltages used in this work. The strong couple of the polarization with the lattice might be the responsible for this persistent 90° domain structure. Once the rotation of the polarization deforms the coupled crystal lattice, generating great local stress, the formation of a new 90° domain arrangement is a way to relieve this stress, and thus, reduce elastic energy.

An interesting point is that the "written" 90° domains walls obtained with PFM most often are arranged in parallel lines with orientations that are dependent on the direction and amplitude of the applied field. Understanding and controlling this "writing" by PFM is a key topic in ferroelectrics, once domain walls might have different properties from the domains itself [35]. In fact, conductivity of 90° domain walls was proposed in lead titanate (PT) [36] and demonstrated in lead zirconate titanate (PZT) [37]. Among the possible factors that lead to domain wall conductivity, the high tetragonality factor [38] is appointed as playing an important role. The high density of domain walls obtained in our work by PFM writing evidence that the lanthanum-modified lead titanate can be a potential material for other multifunctional application involving domain wall nanoelectronics.

Conclusion

In summary, a qualitative three-dimensional reconstruction of the ferroelectric domain structure of a transparent $(Pb_{0.79}La_{0.21})TiO_3$ ceramic was performed by piezoresponse force microscopy. Results revealed that domain

structures are organized in stripes in two size scales (micro and nanometer) separated by 90° domain walls coexisting with 180° domains. The configuration of this structure is a mix of well-ordered domains (nanoscale 90°) with 180° domains in a labyrinth type organization. The bulk domain configuration was depicted in the scenario of cylindrical domains with irregular bases crossing over 90° domain walls, which reproduces the PFM images obtained in this work.

Different reorientation voltages were observed for the three kinds of domains, which according to a theoretical model of polarization reversal in c/a/c-domain structures [34], correspond to a sample with high polarization anisotropy. In the poling process, the labyrinth structure was destroyed at relative low voltages, and a new configuration of 90° domains (different from the spontaneously formed) was created. This new configuration persists, even after the application of relatively high voltages, avoiding the formation of a single-domain state. This behavior, which is a way to relieve stress generated in poling process, suggests a strong coupling of the polarization with the lattice, corroborating with the high polarization anisotropy hypothesis. Finally, the high density of 90° domain walls created in the PFM writing evidences the potential of the lanthanum-modified lead titanate compounds in multifunctional applications involving domain wall nanoelectronics.

Acknowledgements The authors would like to acknowledge Mr. Francisco J. Picon for the technical assistance, and CAPES, CNPq, and FAPESP (#2008/04025-0 and #2013/03118-2) for the financial support.

References

1. Arlt G (1990) Twinning in ferroelectric and ferroelastic ceramics: stress relief. J Mater Sci 25:2655–2666
2. Arlt G, Sasko P (1980) Domain configuration and equilibrium size of domains in BaTiO3 ceramics. J Appl Phys 51:4956–4960
3. Gruverman A, Auciello O, Tokumoto H (1998) Imaging and control of domain structures in ferroelectric thin films via scanning force microscopy. Annu Rev Mater Sci 28:101–123
4. Balke N, Bdikin I, Kalinin SV, Kholkin AL (2009) Electromechanical imaging and spectroscopy of ferroelectric and piezoelectric materials: state of the art and prospects for the future. J Am Ceram Soc 92:1629–1647
5. Gruverman A, Kalinin SV (2006) Piezoresponse force microscopy and recent advances in nanoscale studies of ferroelectrics. J Mater Sci 41:107–116
6. Ivry Y, Chu DP, Durkan C (2010) Bundles of polytwins as metaelastic domains in the thin polycrystalline simple multi-ferroic system PZT. Nanotechnology 21:065702
7. McGilly LJ, Schilling A, Gregg JM (2010) Domain bundle boundaries in single crystal $BaTiO_3$ lamellae: searching for naturally forming dipole flux-closure/quadrupole chains. Nano Lett 10:4200–4205
8. Kalinin SV, Morozovska AN, Chen LQ, Rodriguez BJ (2010) Local polarization dynamics in ferroelectric materials. Rep Prog Phys 73:056502
9. Gruverman A, Rodriguez BJ, Dehoff C et al (2005) Direct studies of domain switching dynamics in thin film ferroelectric capacitors. Appl Phys Lett 87:082902
10. Gruverman A, Wu D, Fan H-J et al (2008) Vortex ferroelectric domains. J Phys 20:342201
11. Kalinin SV, Rodriguez BJ, Jesse S et al (2006) Vector piezoresponse force microscopy. Microsc Microanal 12:206–220
12. Harnagea C, Pignolet A, Alexe M, Hesse D (2002) Piezoresponse scanning force microscopy: what quantitative information can we really get out of piezoresponse measurements on ferroelectric thin films. Integr Ferroelectr 44:113–124
13. Iijima K, Takayama R, Tomita Y, Ueda I (1986) Epitaxial growth and the crystallographic, dielectric, and pyroelectric properties of lanthanum-modified lead titanate thin films. J Appl Phys 60:2914–2919
14. Zhao Q, Liu Y, Shi W et al (1996) Nonlinear optical properties of lanthanum doped lead titanate thin film using Z-scan technique. Appl Phys Lett 69:458–459
15. Londono FA, Eiras JA, Garcia D (2012) Optical and electro-optical properties of (Pb, La)TiO_3 transparent ceramics. Opt Mater 34:1310–1313
16. Londono FA, Eiras JA, Garcia D (2012) Optical and electro-optical characteristics of hot-pressing $(Pb_{1-x}La_x)TiO_3$ ferroelectric ceramics. Bol Soc Esp Cerám Vidr 51:353–358
17. Yamamoto T, Sakamoto J, Saito M, Niori H (2000) Domain structures of $PbTiO_3$ single crystal and La-modified $PbTiO_3$ thin film by kelvin force microscope. In: Proceedings of the ISAF 2000. 12th IEEE international symposium on aplication on ferroelectrics, vol. 2, pp 975–978
18. Liu H, Gong X, Liang J, et al (2006) The domain structure and pyroelectric properties of (111) preferred oriented PLT thin films prepared by RF magnetron sputtering. In: Proceedings of the ISAF 2006. 15th IEEE international symposium on the applications of ferroelectrics, pp 299–302
19. Shvartsman VV, Pertsev NA, Herrero JM et al (2005) Nonlinear local piezoelectric deformation in ferroelectric thin films studied by scanning force microscopy. J Appl Phys 97:104105
20. Poyato R, Calzada ML, Shvartsman VV et al (2004) Direct characterization of nanoscale domain switching and local piezoelectric loops of (Pb, La)TiO3 thin films by piezoresponse force microscopy. Appl Phys A 81:1207–1212
21. Dai X, Xu Z, Viehland D (1996) Normal to relaxor ferroelectric transformations in lanthanum-modified tetragonal-structured lead zirconate titanate ceramics. J Appl Phys 79:1021–1026
22. Randall CA, Rossetti GA, Cao W (1993) Spatial variations of polarization in ferroelectrics and related materials. Ferroelectrics 150:163–169
23. Rossetti GA, Cao W, Randall CA (1994) Microstructural characteristics and diffuse phase transition behavior of lanthanum-modified lead titanate. Ferroelectrics 158:343–350
24. Bastos WB (2011) Domínios ferroelétricos em cerâmicas e materiais nanoestruturados: Investigação por microscopia de piezoresposta. PhD Dissertation, Universidade Federal de São Carlos
25. Shvartsman VV, Dkhil B, Kholkin AL (2013) Mesoscale domains and nature of the relaxor state by piezoresponse force microscopy. Annu Rev Mater Res 43:423–449
26. Shvartsman VV, Kholkin AL (2007) Evolution of nanodomains in $0.9PbMg_{1/3}Nb_{2/3}O_3$-$0.1PbTiO_3$ single crystals. J Appl Phys 101:064108
27. Zhao KY, Ruan W, Zeng HR et al (2014) Domain dynamics of La-doped PMN-PT transparent ceramics studied by piezoresponse force microscope. Appl Surf Sci 293:366–370
28. Zhao KY, Zhao W, Zeng HR et al (2015) Tip-bias-induced domain evolution in PMN–PT transparent ceramics via piezoresponse force microscopy. Appl Surf Sci 337:125–129

29. Bai F, Li J, Viehland D (2005) Domain engineered states over various length scales in (001)-oriented $Pb(Mg_{1/3}Nb_{2/3})O_{3-}x$ $\%PbTiO_3$ crystals: electrical history dependence of hierarchal domains. J Appl Phys 97:054103
30. Moreira EN (1996) Transição de fase difusa e comportamento relaxor em materiais ferroelétricos cerâmicos. PhD Dissertation, Universidade Federal de São Carlos
31. DeVries RC, Burke JE (1957) Microstructure of barium titanate ceramics. J Am Ceram Soc 40:200–206
32. Lehnen P, Dec J, Kleemann W (2000) Ferroelectric domain structures of $PbTiO_3$ studied by scanning force microscopy. J Phys D Appl Phys 33:1932–1936
33. Rossetti GA, Khachaturyan AG, Akcay G, Ni Y (2008) Ferroelectric solid solutions with morphotropic boundaries: vanishing polarization anisotropy, adaptive, polar glass, and two-phase states. J Appl Phys 103:114113
34. Ishibashi Y, Iwata M, Salje E (2005) Polarization reversals in the presence of 90° domain walls. Jpn J Appl Phys 44:7512–7517
35. Catalan G, Seidel J, Ramesh R, Scott JF (2012) Domain wall nanoelectronics. Rev Mod Phys 84:119–156
36. Meyer B, Vanderbilt D (2002) Ab initio study of ferroelectric domain walls in $PbTiO_3$. Phys Rev B 65:104111
37. Feigl L, Yudin P, Stolichnov I et al (2014) Controlled stripes of ultrafine ferroelectric domains. Nat Commun 5:4677
38. Freitas VF, Protzek OA, Montoro LA et al (2013) A phenomenological model for ferroelectric domain walls and its implications for $BiFeO_3$–$PbTiO_3$ multiferroic compounds. J Mater Chem C 2:364–372